PROCEEDINGS, Thirty-Sixth Workshop on Geothermal Reservoir Engineering
Stanford University, Stanford, California, January 31 - February 2, 2011
SGP-TR-191

# GEOLOGY AND HYDROTHERMAL ALTERATION OF THE RAFT RIVER GEOTHERMAL SYSTEM, IDAHO

Clay Jones
Joseph Moore
William Teplow
Seth Craig

Energy & Geoscience Institute at the University of Utah
423 Wakara Way Suite 300
Salt Lake City, Utah, 84108, USA
e-mail: cjones@egi.utah.edu

## ABSTRACT

The Raft River geothermal system is located in southern Idaho, near the Utah-Idaho state boarder in the Raft River Valley. The field, which is owned and operated by U.S. Geothermal, has been selected as an EGS demonstration site by the U. S. Department of Energy. This paper summarizes ongoing geologic and petrologic investigations being conducted in support of this project.

The reservoir is developed in fractured Proterozoic schist and quartzite, and Archean quartz monzonite cut by younger diabase intrusions. The basement complex was deformed during the mid Tertiary and covered by approximately 5000 ft of late Tertiary sedimentary and volcanic deposits. Listric normal faults of Cenozoic age disrupt the Tertiary deposits but do not offset the basement rocks.

RRG-9, the target well, was drilled southwest of the main well field to a measured depth (MD) of 6089 ft. The well is deviated to the west and cased to a depth of 2316 ft MD. It penetrated the Proterozoic reservoir rocks at a depth of 5286 ft MD and encountered a maximum temperature of 139 degrees C. Bottom-hole temperatures in other deep wells range from 133 to 149 degrees C.

X-ray diffraction and thin section analyses are being conducted on samples from 5 deep wells, RRG- 1, 2, 3, 7 and 9, to determine the characteristics of the rock types and hydrothermal alteration within the geothermal system. Thin section analyses of samples from RRG-9 document the presence of strong alteration and brecciation at the contact between the Tertiary and basement complex. The Tertiary rocks consist of ash-flow tuffs, lava flows, tuffaceous siltstone, greywacke, and sandstone.

No core is available from RRG-9 but core was obtained from RRG-3C. The sample is a brecciated and altered siltstone from the base of the Tertiary sequence and is similar to rocks at the base of the Tertiary deposits in RRG-9. The results of thermal and quasi-static mechanical property measurements that were conducted on the core sample are presented.

## INTRODUCTION

The Raft River Enhanced Geothermal System (EGS) project is a cooperative effort between the U. S. Department of Energy, the Energy & Geoscience Institute/University of Utah, U.S. Geothermal Inc. and Apex HiPoint Reservoir Engineering. The primary objective of this project is to improve the performance of the Raft River geothermal field by improving the permeability of RRG-9, drilled to the south of the main bore field.

The Raft River geothermal system is located 90 miles southwest of Pocatello, near the Utah-Idaho state boarder in the Raft River Valley (Figure 1). The valley lies at approximately 4800 ft MSL. The geothermal resource was discovered when two agricultural wells, the Bridge and Crank wells encountered boiling water sometime prior to 1950. Geothermometer temperatures indicated a resource with a temperature of 300$^{o}$F.

Since 1973, 34 auger holes to 100 ft depth, 5 core holes from 250 to 1423 ft depth, (Crosthwaite, 1976), 9 deep full diameter and 7 monitoring wells from 500 to 1300 ft depth have been drilled. The production and injection wells were drilled to depths ranging

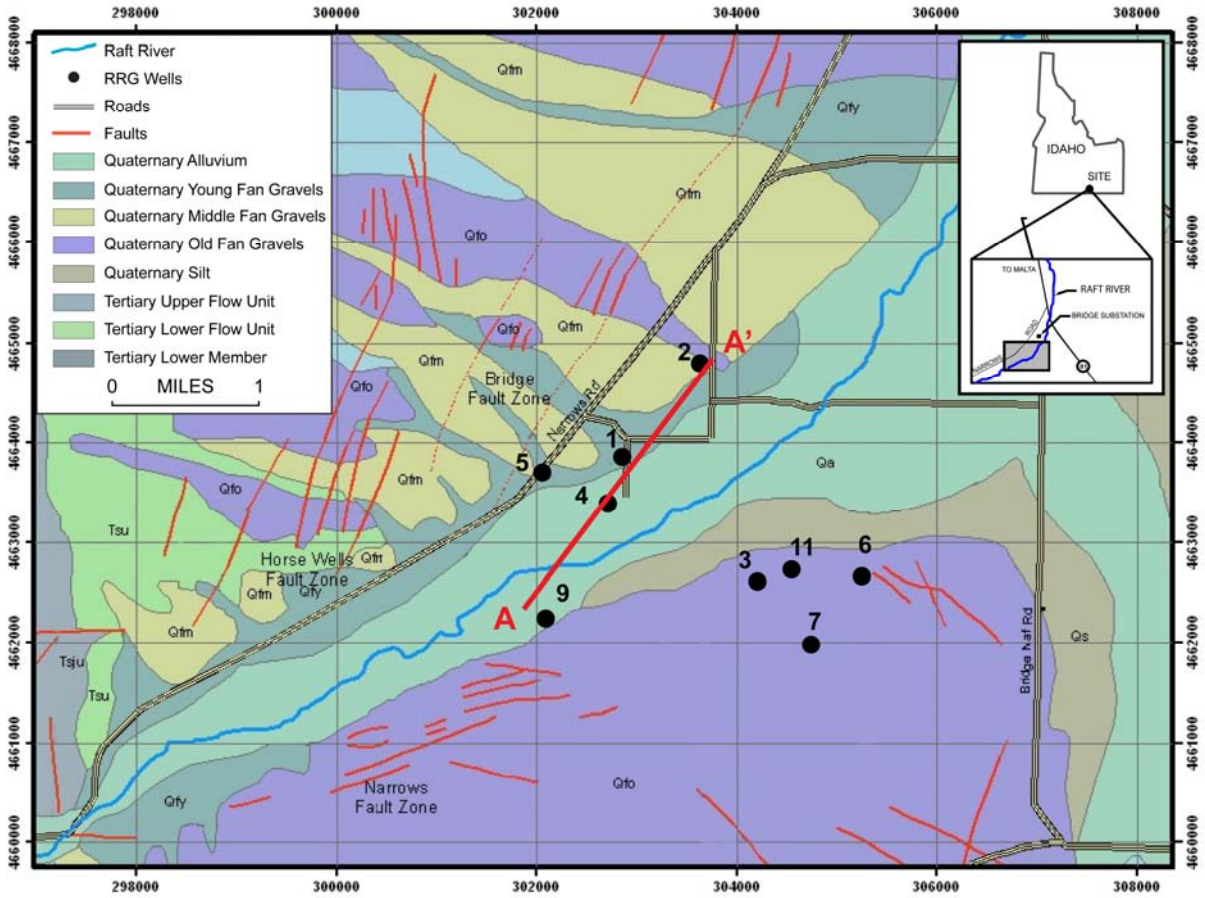


*Figure1: Geologic map of the Raft River Geothermal Field, with inset map showing general location, and line A to A' is the location of the cross-section shown in Figure 5.*

from 3844 to 6540 ft. Wells RRG-1, 2, 4, and 7 are currently being used as production wells; RRG-3, 6, and 11 as injection wells (Figure 1). The production wells record bottom hole temperatures ranging from 133$^{o}$ to 149$^{o}$C. The produced fluids are NaCl waters with total dissolved solid contents ranging from 1465 to 4059 ppm (Dolenc et al., 1981).

The major structure in the Raft River Geothermal area is a regional (100s of km$^2$), normal, low-angle, detachment fault separating ductilly deformed Proterozoic and Archean rocks from Tertiary ash-flow tuffs, rhyolite flows and basin-filling sediments. Movement along this structure occurred from about 20 to 40 Ma (Williams et al., 1982 and Covington, 1983). The detachment fault transported Paleozoic Rocks to the east (Black Pine Mountains.) away from the rising gneiss dome in the west (Albion Mountains). Roughly 24 kms of slip has occurred along the detachment (Wells, 2001). The detachment fault, the ductilly deformed rocks of the footwall and the brittle deformation of the hanging wall (Paleozoic) are exposed in the Raft River Range to the south of the geothermal area. There are no major normal faults along the range fronts in the Raft River Basin, offset is generally less than 200m (Pierce et al., 1983).

Normal faults to the North and West of the Geothermal Field cut the Quaternary deposits and define the Bridge and Horse Well Fault Zones (Figure 1) (Williams et al., 1974, 1976). The faults appear to be steeply dipping at shallow depths. However, televiewer logs from RRG-4 and 6 document fractures with dips ranging from nearly vertical to as little as 6$^{o}$. In general, the degree of fracturing increases with depth while the dip of the fractures decreases (Covington, 1980). This observation led Covington (1980) to conclude that the Tertiary and Quaternary faults sole out along the top of the Proterozoic and Archean basement complex and that the basement rocks and Tertiary rocks are structurally detached from each other. This interpretation is consistent with the lack of major structural offsets of the basement complexe indicted by seismic data (Ackerman, 1979) and the analysis of rock samples from the deep wells (Covington, 1980).

The Bridge and Horse Well Fault Zones appear to terminate southward at a poorly understood structure

referred to as the Narrows Structure. This structure is interpreted to be a right lateral strike slip basement shear (Mabey et al., 1978). The location of the deep upflow zone of the geothermal system is thought to be controlled by the intersection of the Bridge Zone with the Narrows structure.

The Jim Sage and Cotterell Mountains are primarily composed of rhyoite erupted 9 to 10 Ma (Williams et al., 1982) and are the source of the ash-flow tuffs, lava flows and volcaniclastic sediments infilling much of the basin. Subsequent volcanic activity is represented by two small rhyolite domes emplaced within the Raft River valley. Round Mountain was emplaced at 8.3 $\pm$ 1.7 Ma west of the Black Pine Mountains. Sheep Mountain was emplaced on the east side of the Jim Sage Mountains at 8.42 $\pm$ 0.2 Ma (Dolenc et al., 1981)

## THE TARGET WELL, RRG-9

RRG-9 was drilled in 2006 to a measured depth (MD) of 6089 ft southwest of the main well field. The location was selected to test the southern extension of the productive fracture zone associated with the production interval in RRG-7. Fluid production is primarily from fractures in the Proterozoic Elba Quartzite (see discussion below), a fine-grained rock with low porosity. The well is deviated to the west with a 44$^{o}$ inclination at its base. It penetrated the Proterozoic reservoir rocks at a depth of 5286 ft MD beneath the Tertiary Salt Lake Formation. The well encountered permeability at shallow depth but did not encounter commercial permeability within the main reservoir units. Prior to the stimulation, the well will be cased to the top of the Elba Quartzite at a depth of 5430 ft MD.

## PETROGRAPHIC INVESTIGATION

Thirty-seven samples of cuttings from well RRG-9 have been selected for X-ray diffraction and Petrographic study. Samples were selected approximately every 300' from 290'-300' to 4800'-4810', and approximately every 50' from 5100'-5150' to the bottom of the well at 6070'-6080'. All sample depths discussed in this section are measured depths. Petrographic observations are grouped by formation/member and can be found below.

### X-Ray Diffraction

Changes in both clay and zeolite minerals can be seen with depth in the X-ray diffraction data. The transition from smectite to interlayerd illite/smectite occurs at relatively shallow depth (between 600' and 900') (Figure 2). The transition from interlayered chlorite/smectite to chlorite occurs near the base of the well. Zeolite minerals (Figure 3) change from clinoptilolite to analcime to laumonite with depth.

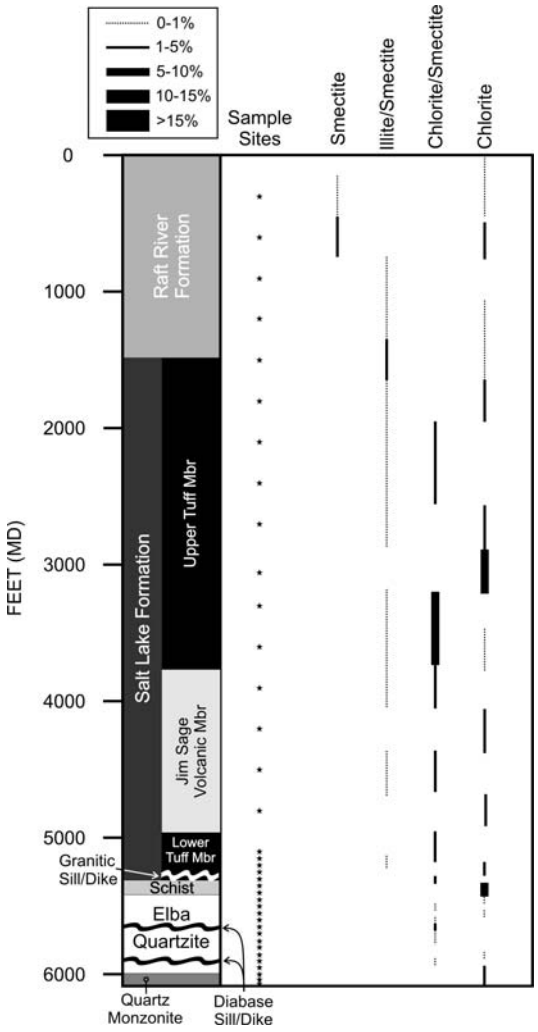


*Figure 2: Clay mineralogy with depth for well RRG-9. Litholgic column is shown at the left hand side, along with a depth scale. The Quartzite of Yost at the top of the basement complex is too thin to show. Sample depths are denoted by a star. Weight percent of the sample is indicated by the width of the line with a legend at the upper left.*

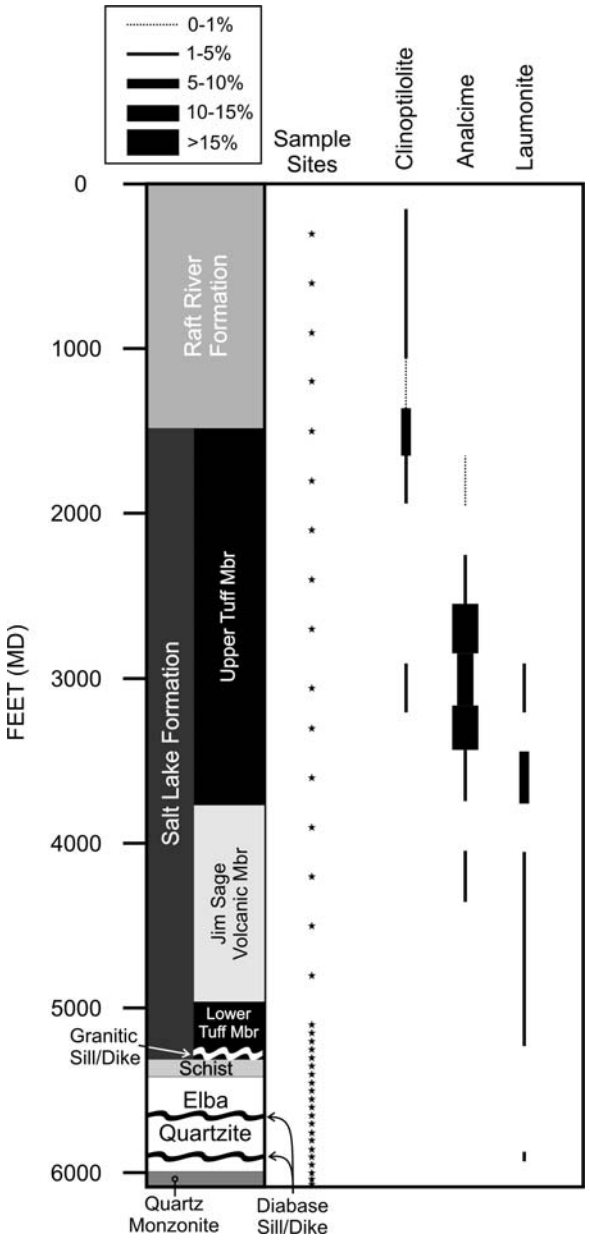


*Figure 3: Zeolite mineralogy with depth for well RRG-9. Litholgic column is shown at the left hand side, along with a depth scale. The Quartzite of Yost at the top of the basement complex is too thin to show. Sample depths are denoted by a star. Weight percent of the sample is indicated by the width of the line with a legend at the upper left.*

**Raft River Formation**

The Raft River Formation consists of conglomerates, sandstones and siltstones composed of angular, poorly-sorted lithic clasts. Lithic clasts include quartzites, granites, lava flows, ash-flow tuffs and fragments of calcite. Degree of diagenesis is variable and ranges from clast supported and poorly cemented to clay matrix supported

**Salt Lake Formation**

***Upper Tuffaceous Member***

The Salt Lake Formation ranges in age from greater than 11 to 2-3 Ma (Williams et al., 1982). The upper tuffaceous member is composed of sandstones, siltstones, shales and ash-flow tuffs. The sandstones are immature, poorly sorted and poorly rounded. They are primarily lithic wackes. Siltstones and shales are often rich in carbonate, possibly reflecting a lacustrine depositional environment. The ash-flow tuffs are generally lithic and crystal poor, and poorly welded, and altered to zeolite, quartz and chalcedony and calcite. Calcite is the primary vein and vug filling mineral.

***Jim Sage Volcanic Member***

Glassy to devitrified rhyolite flows, with resorbed/skeletal plagioclase phenocrysts. Silicification is most intense in the upper portion and decreases with depth. Paragnesis of open-space-filling minerals: 1) chalcedony; 2) quartz; 3) calcite; and 4) laumontite.

***Lower Tuffeceous Member***

The Lower Tuffaceous Member is primarily composed of poorly welded, crystal and lithic poor ash-flow tuffs. Minor rhyolite flows are found in the upper portion of the unit. Fragments of Proterozoic and Archean quartzite and intrusive rocks are found near the base. Traces of calcite and titanite are observed in the upper portions of the unit. The lowermost portions (5250'-5260' and 5300'-5310') are strongly brecciated and indurated above the contact with the Proterozoic and Archean rocks. Veining becomes more common as the contact is approached; veins are entirely filled with quartz, adularia and calcite or partially filled by laumonite and calcite. Traces of quartzite are found in the lower 2 samples, this may be the Quartzite of Yost, which is not otherwise seen in thin-section. Approximately one third of the bottom most sample (5300'-5310') consists of an intrusive composed of plagioclase, microcline, quartz, clinopyroxene, and biotite.

**Proterozoic and Archean basement complex**

The basement complex rocks consist of 5 units within the Raft River Geothermal Field. The upper most unit, the Quartzite of Yost is less than 20 ft thick in RRG-9, and is not shown in the figures. It is represented in thin-section by a few chips of clean white quartzite. The underlying units include the Upper Narrow Schist, the Elba Quartzite (EGS target formation), the Lower Narrows Schist, and Quartz

Monzonite. In addition dikes of diabase were encountered within the Elba Quartzite.

***Upper Narrows Schist***

The Upper Narrows Schist consists of ductilly sheared quartz, K-feldspar, muscovite, biotite, with minor chlorite veining and alteration, and traces of calcite veins.

***Elba Quartzite***

The Elba Quartzite is a ductilly sheared quartzite. The quartz grains display undulatory extinction, with locally common muscovite and K-feldspar. Diabase intrusives are found at 5650'-5660' and 5900'-5910', they display minor brecciation, but no significant shearing suggesting they postdate the formation of the metamorphic core complex that affected the Proterozoic and Archean rocks. The diabase is composed of plagioclase, clinopyroxene, amphibole, magnetite and biotite. Some of the ferromagnesian minerals are altered to interlayered chlortite/smectite. At 5650'-5660' the matrix contains fine-grained K-feldspar. The degree of brecciation and the abundance of veins in the country rock increases as the intrusions are approached.

***Lower Narrows Schist***

The Lower Narrows Schist is a quartz, muscovite schist that displays minor brecciation, and is cut by minor calcite and chlorite veins. The rock also displays evidence of ductile shearing.

***Quartz Monzonite***

The Quartz Monzonite consists of quartz, K-feldspar, plagioclase muscovite and biotite, with traces of titanite and epidote. Traces of brecciation and calcite veins are present. Chlorite replaces biotite and epidote replaces plagioclase. As with the other Proterozoic and Archean rocks evidence of ductile shearing is observed in the cuttings.

## MECHANICAL TESTING OF CORE

No core is available from RRG-9 for mechanical testing or from the basement rocks from other wells. Core samples from the overlying rocks were however, collected during the drilling of the original wells under the DOE program. The deepest of the core samples suitable for testing was obtained from RRG-3C at a depth of 5270-5272 ft. The rock is a brecciated siltstone containing abundant ostracod fossils. X-ray diffraction analyses indicate the rock contains approximately 31% quartz, 2% plagioclase, 49% K-feldspar, 7% calcite, 5% muscovite and illite and 6% interlayered chlorite-smectite. Some of the K-feldspar and quartz are interpreted to be secondary in origin.

In-situ mechanical properties – strength at in-situ confining pressure as well as static and dynamic values for Young's modulus and Poisson's ratio under the same conditions were measured on two pieces of the core (EGM 1-2 and EGM 2-4). Tensile strength was also assessed using Brazilian testing on disks oriented parallel, perpendicular and at 45° to the axis of the core. The triaxial compression tests at inferred in-situ conditions are shown in Table 1.

*Table 1: Summary of Triaxial Tests Raft River*

| Sample ID | EGM 1-2 | EGM 2-4 |
|---|---|---|
| Depth (ft) | 5270 | 5271.9 |
| Saturated Bulk Density ($g/cm^3$) | 2.385 | 2.215 |
| Effective Confining Pressure (psi) | 2020 | 2020 |
| Effective Compressive Strength (psi) | 12,855 | 9720 |
| Effective Residual Compressive Strength (psi) | 8635 | 8325 |
| Quasi-Static Young's Modulus (psi) | 2,824,000 | 1,767,000 |
| Quasi-Static Poisson's Ration | 0.15 | 0.15 |

The Terzaghi effective confining pressure was calculated based on a pressure gradient of 0.38 psi/ft, a vertical stress gradient of 1.04 psi/ft, a maximum horizontal stress gradient of 0.85 psi/ft and a minimum horizontal stress gradient of 0.62 psi/ft. Figure 4 shows comparative stress-strain data for this material. This figure shows the axial stress difference ($\sigma_1 - \sigma_3$) versus average radial and axial strain. If the effective confining pressure $\sigma'_3$ is added to the axial stress difference, the effective compressive strength is estimated for each sample at nominally representative in-situ conditions. The effective residual compressive strength is the strength of the specimen after peak loading and some degree of stabilization. Figure 4 shows behavior representative of perfect plasticity after failure. This ductility may be attributed to a degree of brecciation in the core sample. Dynamic mechanical properties were also inferred from high frequency acoustic transmisiion measurements. These data are shown in Table 2. In most instances Young's moduli determined acoustically will exceed those determined using pseudostatic loading to failure. Other testing carried include scratch testing, to infer the potential variation of properties along the length of the small sample available, and thermal properties determinations.

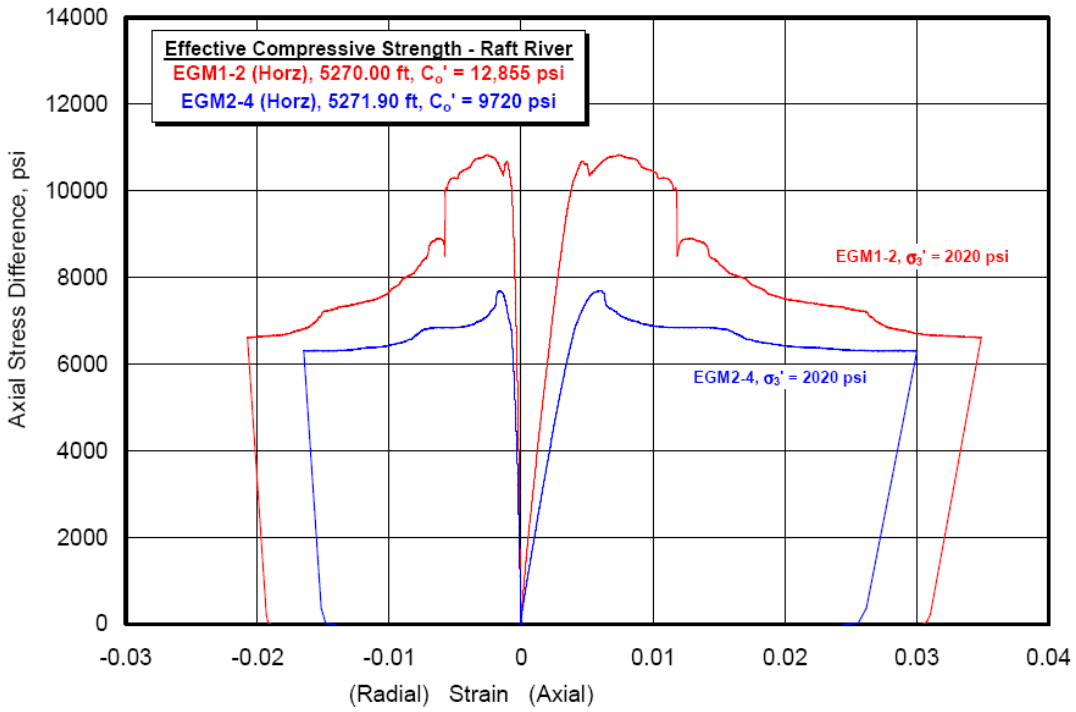


*Figure 4. Summary plot of the stress-strain response for two Raft River samples (saturated with 0.4% NaCl) at 140º C, depth 5270.00 – 5271.90 ft. The effective compressive strength for each test is indicated in the figure. The axial stress difference is the difference between the applied axial stress and the confining pressure.*

The thermal conductivity of the core samples were determined under a confining pressure of 2120 psi and a pore pressure of 100 psi. The samples were saturated with a 0.4% NaCl solution. The results of those tests are reproduced and show that the thermal conductivity of sample EGM1-1 varies over temperature from 1.775 to 1.929 W/m-K with an average value of 1.851 W/m-K; Thermal conductivity of EGM2-5 varies with temperature from 1.210 to 1.315 W/m-K with an average value of 1.227 W/m-K (Table 2).

*Table 2. Summary of the thermal conductivity of core samples.*

| Sample ID | Well Depth (ft) | Average Test Temperature (°C) | Average Thermal Conductivity (W/m-K) |
|---|---|---|---|
| EGM 1-1 | 5270.1 | 34 | 1.775 |
| | | 68 | 1.850 |
| | | 138 | 1.929 |
| | | Average over all Temp. | 1.851 |
| EGM 2-5 | 5272.15 | 33 | 1.210 |
| | | 70 | 1.307 |
| | | 134 | 1.315 |
| | | Average over all Temp. | 1.277 |

The coefficient of thermal expansion was evaluated on two samples of the core (Table 3). This parameter is important for predicting changes in the in-situ stresses and the potential for the dendritic thermal fracture growth. The results of the tests are included in Table 3.

*Table 3: Results from Axial Thermal Expansion Testing*

| Sample ID | Depth | Average $\alpha_{axial}$ For 30 to 70°C ($10^{-6}$/°C) | Average $\alpha_{axial}$ For 70 to 140°C ($10^{-6}$/°C) |
|---|---|---|---|
| EGM 1-3 | 5,270.00 | 8.80 | 14.17 |
| EGM 2-3 | 5,272.05 | 4.84 | 9.04 |

## CONCLUSIONS

The following conclusions can be drawn from this study:

1. The stratigraphy of the rocks encountered in RRG-9 is similar to those in other deep wells of the field (Figure 5). The well encountered approximately 4800 ft of Quaternary and Tertiary deposits above the Proterozoic and Archean basement rocks.

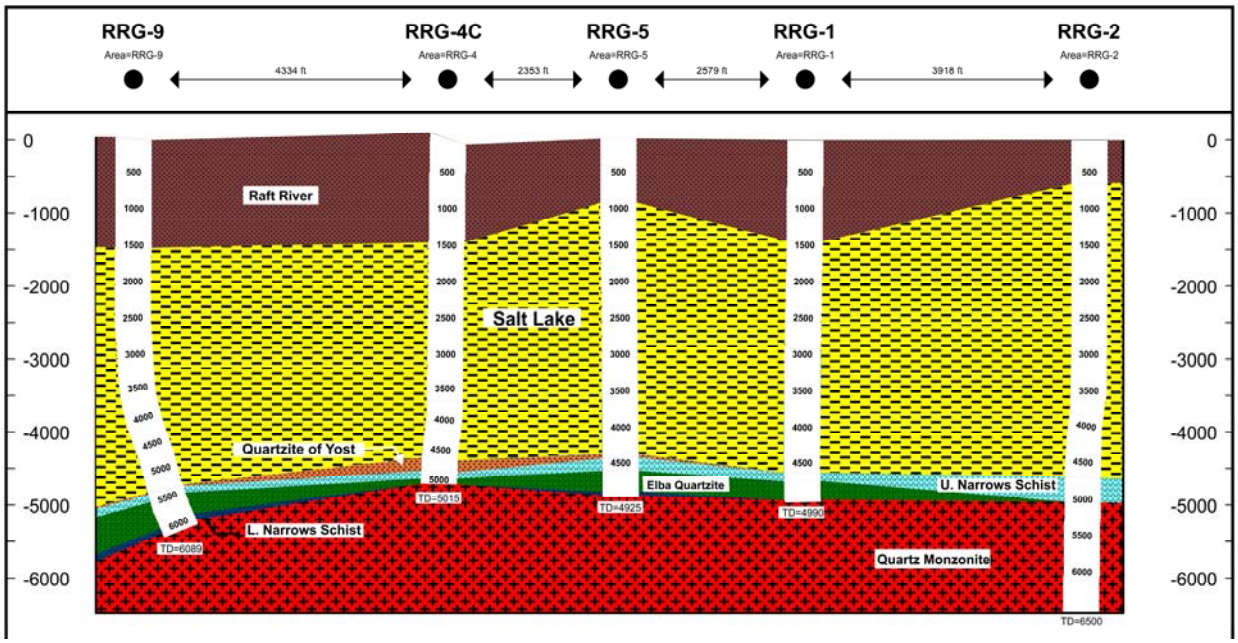


*Figure 5. Southwest to northeast cross-section of the Raft River Geothermal Field. Location of cross-section shown on Figure 1.*

2. The Tertiary deposits consist of upper and lower sequences of ash-flow tuffs and volcaniclastic deposits separated by rhyolite lava flows (Figures 2 and 3). Alteration and brecciation generally increase downward as the basement contact is approached, with the lower volcanic sequence most intensely altered. Silica and K-feldspar flooding and replacement of the volcanic glass by zeolites is common. Vein filling minerals include quartz, chalcedony, adularia, zeolites, and calcite. The youngest veins are partially filled with zeolites and calcite, suggesting alteration occurred at temperatures consistent with the present temperatures of about 140$^{o}$C.

3. The basement rocks include schists, quartzite and quartz monzonite that display intense ductile shearing. This basement complex is cut by weakly altered diabase.

4. The depth to the basement complex is similar to that found in other deep wells implying that there are no major offsets of the Tertiary-basement contact between RRG-9 and the main portion of the bore field (Figure 5).

## ACKNOWLEDGEMENTS

We would like to thank the management and staff of U. S. Geothermal Inc. for generously providing samples and data used in this investigation and for their support in all phases of the study. Funding was provided by the U. S. Department of Energy under contract DE-FG36-08GO18189.

## REFERENCES

Ackerman, H. D. (1979) Seismic refraction study of the Raft River geothermal area, Idaho. Geophysics, 44, 216-255

Crosthwaite, E. G. (1976) Basic data from five core holes in the Raft River geothermal area, Cassia County, Idaho, U. S. Geological Survey Open-File Report 76-665, 12.

Covington, H.R. (1980) Subsurface geology of the Raft River geothermal area. Geothermal Resources Council Transactions, 4, 113-115.

Covington, H.R. (1983 )Structural evolution of the Raft River basin Idaho in Tectonic and Stratigraphic Studies in the Eastern Great Basin. Memoir 157, Geological Society of America, 229-237.

Dolenc, M.R., Hull, L.C., Mizell, S.A,, Russell, B.F., Skiba P.A., Strawn, J.A. and Tullis, J.A., (1981) Raft River Geoscience Case Study. EG&E Idaho Report EGG-2151.

Mabey, D. R., Hoover, D. B., and J. E. O'Donnell (1978) Reconnaissance geophysical studies of the geothermal system in southern Raft River Valley, Idaho. Geophysics, 43(7), 1470-1484.

Pierce, K. L., Covington, P. L., Williams, and D. H. McIntyre (1983) Geologic Map of the Cotterel Mountains and northern Raft River Vally, Idaho. U.S. Geological Suryey Miscellaneous Geologic Investigation Map I-1450.

Wells, M. L. (2001) Rheological control on the initial geometry of the Raft River detachment fault and shear zone, western United States. Tectonics, 20(4), 435-457.

Williams, P. L., Covington, H. R., and K. L. Pierce (1982) Conozoic Stratigraphy and Tectonic Evolution of the Raft River Basin, Idaho. In Bill Bonnichsen and R.M. Breckenridge, eds. Conozoic Geology of Idaho: Idaho Bureau of Mines and Geology Bulletin 26, 491-504.

Williams, P.L., Mabey, D.R., Zohdy, A.R., Ackerman, H.D., Hoover, D.B., Pierce, K.L., and Oriel, S.S. (1976) Geology and geophysics of the southern Raft River valley geothermal area, Idaho, USA: Proceeding, Second United Nations Symposium on the Development and Use of Geothermal Resources, San Francisco, May 1975, 2, 1273-128.

Williams, P.L., Pierce, K.L., McIntyre, D.H. and Schmidt, P.W. (1974) Preliminary geologic map of the southern Raft River valley, Cassia County, Idaho: U.S. Geological Survey Open File Report.